Frequency selectivity of the human cochlea

Manley, Geoffrey A.; van Dijk, Pim

Published in:
Hearing Research

DOI:
10.1016/j.heares.2016.04.004

Hearing Research 336 (2016) 53–62

Contents lists available at ScienceDirect

Hearing Research

journal homepage: www.elsevier.com/locate/heares

Research paper

Frequency selectivity of the human cochlea: Suppression tuning of spontaneous otoacoustic emissions

Geoffrey A. Manley [a], Pim van Dijk [b, c, *]

[a] Cochlear and Auditory Brainstem Physiology, Department of Neuroscience, School of Medicine and Health Sciences, Cluster of Excellence "Hearing4all", Research Centre Neurosensory Science, Carl von Ossietzky University Oldenburg, 26129 Oldenburg, Germany
[b] University of Groningen, University Medical Center Groningen, Department of Otorhinolaryngology/Head and Neck Surgery, P.O. Box 30.001, 9700 RB Groningen, The Netherlands
[c] University of Groningen, Graduate School of Medical Sciences, Research School of Behavioural and Cognitive Neuroscience, The Netherlands

ARTICLE INFO

Article history:
Received 12 January 2016
Received in revised form
25 March 2016
Accepted 15 April 2016
Available online 29 April 2016

Keywords:
Human hearing
Frequency selectivity
Otoacoustic emissions

ABSTRACT

Frequency selectivity is a key functional property of the inner ear and since hearing research began, the frequency resolution of the human ear has been a central question. In contrast to animal studies, which permit invasive recording of neural activity, human studies must rely on indirect methods to determine hearing selectivity. Psychophysical studies, which used masking of a tone by other sounds, indicate a modest frequency selectivity in humans. By contrast, estimates using the phase delays of stimulus-frequency otoacoustic emissions (SFOAE) predict a remarkably high selectivity, unique among mammals. An alternative measure of cochlear frequency selectivity are suppression tuning curves of spontaneous otoacoustic emissions (SOAE). Several animal studies show that these measures are in excellent agreement with neural frequency selectivity. Here we contribute a large data set from normal-hearing young humans on suppression tuning curves (STC) of spontaneous otoacoustic emissions (SOAE). The frequency selectivities of human STC measured near threshold levels agree with the earlier, much lower, psychophysical estimates. They differ, however, from the typical patterns seen in animal auditory nerve data in that the selectivity is remarkably independent of frequency. In addition, SOAE are suppressed by higher-level tones in narrow frequency bands clearly above the main suppression frequencies. These narrow suppression bands suggest interactions between the suppressor tone and a cochlear standing wave corresponding to the SOAE frequency being suppressed. The data show that the relationship between pre-neural mechanical processing in the cochlea and neural coding at the hair-cell/auditory nerve synapse needs to be reconsidered.

1. Introduction

For decades, the frequency selectivity of the human hearing organ could only be assessed using indirect methods, such as the masking of tones by other tones or by noise, evaluating the perceptions of human subjects (Glasberg and Moore, 1990). The results of these psychophysical techniques, however, depended on the specific suppression-stimulus patterns used. Typically, results from tonal masking experiments produce a different frequency selectivity when in simultaneous-, rather than forward-masking, mode and both depend on the sound pressure levels of the stimuli (Eustaquio-Martin and Lopez-Poveda, 2010; Lopez-Poveda and Eustaquio-Martin, 2013). Thus the data obtained using these methods were not conclusive.

Since their discovery, otoacoustic emissions, faint sounds emitted by the ear spontaneously or induced by sound stimuli, have made it possible to use non-invasive objective techniques to study human hearing (Kemp, 1978; Zurek, 1981). One type of emission is the stimulus-frequency otoacoustic emission (SFOAE) that is emitted as the result of a single tonal frequency stimulus. Their magnitude and phase can be measured by observing the effects of adding a second tone that is close in frequency and of a slightly higher level. The results in human ears suggest that the SFOAE phase rolls off at a very high rate. This has been interpreted to mean that the frequency selectivity of the system is very high, indeed

* Corresponding author. University of Groningen, University Medical Center Groningen, Department of Otorhinolaryngology/Head and Neck Surgery, P.O. Box 30.001, 9700 RB, Groningen, The Netherlands.
E-mail address: p.van.dijk@umcg.nl (P. van Dijk).

http://dx.doi.org/10.1016/j.heares.2016.04.004

higher than measured in any other non-specialized mammal (Shera et al., 2002, 2010). Frequency selectivity so assessed is, at higher frequencies, at least twice as high as that measured using psychophysical techniques (Glasberg and Moore, 1990; Lopez-Poveda and Eustaquio-Martin, 2013). These two opposing data sets have so far dominated the discussion in the literature (Bergevin et al., 2012; Lopez-Poveda and Eustaquio-Martin, 2013; Ruggero and Temchin, 2005; Siegel et al., 2005) and it remains unclear whether either data set can indicate the true frequency selectivity of single fibers of the human auditory nerve that represent the stimulus input to auditory brain centers.

Spontaneous otoacoustic emissions (SOAE) offer an additional method of assessing frequency tuning selectivity, especially since humans and other primates generally show unusually large numbers of SOAE when compared to standard laboratory mammals. About 70% of healthy human ears emit SOAE, observable as sharp peaks in the ear canal sound spectrum in quiet (Talmadge et al., 1993). SOAE can be suppressed and, near their own frequency, are sensitive to the presence of near-threshold external tones. Changing the external-tone frequency and observing the levels necessary to elicit a standard level of suppression of a single SOAE peak enables the measurement of suppression tuning curves (STC). Curiously, although a number of older publications report studies of human SOAE patterns, in each study only very few STC were collected, using different suppression criteria and only within a narrow frequency range (Rabinowitz and Widin, 1984; Schloth and Zwicker, 1983; Frick and Matthies, 1988; Zwicker and Peisl, 1990). In general, the frequency selectivity of those STC was moderate and, in that narrow frequency range, roughly comparable to the selectivity observed in invasive animal studies of the auditory nerve (e.g., Liberman, 1978).

Since, in contrast to SFOAE measurements, SOAE arise spontaneously and SOAE-STC tuning selectivity can be measured using single tones near hearing thresholds, the suppression of SOAE is the least complex and most sensitive technique currently available for measuring frequency selectivity in humans. In the Macaque monkey, the only other primate species for which a small sample of SOAE STC is available (Martin et al., 1988), the match to auditory nerve tuning selectivity (Shera et al., 2011) is very good.

In view of the lack of systematic study of the suppression behavior of human SOAE, we examined 63 SOAE covering a wide range of frequencies in 23 healthy ears of 13 young adults (one male and 12 female) under very quiet conditions.

2. Methods

Suppression of spontaneous otoacoustic emissions (SOAEs) was studied in 23 ears of 13 fully awake subjects, of which 12 were female, varying in age from 21 to 30 years (median 23 years). The ears, and hence the subjects, were selected for the presence of one detectable SOAE that could be suppressed by an external tone over at least 8 dB before disappearing into the equipment noise floor. The audiometric thresholds of the ears were better than 20 dB HL at the octave frequencies from 500 to 8000 Hz, as assessed with TDH 38 headphones connected to a clinical audiometer (Equinox, Interacoustics, Denmark).

Spontaneous otoacoustic emissions were recorded using an ER10B high-sensitivity microphone (Etymotic Research Inc., Elk Grove Village, IL, USA) inserted into the ear canal. The emission signals were multiplied 40 dB by the microphone's preamplifier. The signal was filtered by an SR560 low-noise amplifier setup as a high-pass filter (300 Hz cutoff, 12 dB/octave) and by a SR640 low-pass filter (15 kHz cutoff, −115 dB/oct; both filters by Stanford Research, Sunnyvale, California, USA). An insert earphone (Etymotic ER2) was connected to the microphone probe to present auditory stimuli. The filtered microphone signal and the stimulation earphone were both connected to an Audiofire 24-bit AD/DA converter (Echo audio, Santa Barbara, CA, USA) for digital signal recording and generation, respectively. The AD/DA converter was controlled using custom Matlab software (R2014b, Mathworks Inc., Natick, MA, USA) running on an Apple laptop computer.

The recording microphone was calibrated using a condenser microphone B&K 4134 (Brüel & Kjær, Denmark) following the procedure for emission probe calibration described by Siegel (2007). The stimulation earphone was calibrated against a 40AG calibration microphone, in a RA0045 ear simulator (G.R.A.S. Sound & Vibration, Denmark).

Unsuppressed SOAEs were recorded for 120 s, from which an emission spectrum was computed (van Dijk et al., 2011). Suppression of SOAEs was studied by presenting pure tones of duration 1.2 s, and with 10-ms cosine on/off ramps. When a tone was presented, the emission recording started 150 ms prior to the onset of the tone and lasted till 150 ms after offset of the tone. Tone levels ranged from 10 to 70 dB SPL in 3 dB steps. Tone frequencies ranged from 0.5 to 10.0 kHz, in 1/16 octave steps. Thus, a total of 21 levels at 70 frequencies yielded 1470 short 1.5-s sound fragments stored on the experimentation laptop computer for later analysis. The tones were presented in a quasi-random order, as determined by the Matlab routine 'randperm' (random permutation). During these recordings, subjects could follow the progress on a computer screen. Subjects were instructed to be as quiet as possible during the recordings, but were allowed to read a book or an e-reader. Every two minutes there was a 10-s break to allow the subject to cough, swallow or turn the page of their book. These series of measurements took about 41 min per ear, including the 10s breaks. Two subjects had SOAEs above 8 kHz. These we additionally studied in a session where the frequencies ranged from 5000 to 16000 Hz, in 1/16 octave steps, which gave $21 \times 27 = 567$ sound fragments. Here, each series took about 16 min.

To relate the stimulus tone used during suppression experiments to thresholds, individual-ear hearing thresholds were assessed psychoacoustically with the microphone probe in situ, and using stimuli produced by the ER2 insert earphone. Tones had a 300 ms duration and 10 ms cosine rise/fall ramps. Tone frequencies were 0.5 kHz and from 1 to 10 Hz in 1 kHz steps. In the high-frequency measurements performed in two subjects, the tones ranged from 5 to 16 kHz in 1 kHz steps. For each frequency, the tone thresholds were determined in a 3-alternative forced-choice procedure, in which subjects viewed 3 buttons on a computer interface, that were subsequently lit. Subjects indicated during which of the three buttons a tone was heard. Tone levels were controlled in a 1-up-2-down staircase (5 dB step size). The procedure was stopped after 8 reversals. The last 6 reversal levels were averaged to obtain the tone threshold level.

For each ear, a recording session consisted of the following sequence of tests: 1. An SOAE recording without suppressor tones. 2. The threshold measurement. 3. A second SOAE measurement. 4. The SOAE recording with suppressor tones. 5. A third SOAE measurement. During this sequence, the recording probe was not removed from the ear canal.

The spectrum for each ear typically contained several SOAE emission peaks. Suppression of these emission peaks was subsequently analyzed separately for each suppression recording. Suppression recordings consisted of 1470 or 567 brief sound fragments, each of duration 1.5 s (see above). Suppression of an SOAE peak was assessed by an analysis of the center 1 s of such a sound fragment. During the recording of this 1s segment, a suppression tone had been present along with the suppressed SOAE signal. Initially, the suppressor tone was filtered out, by fitting a curve $y(t) = a_1 \cos 2\pi f_s t + b_1 \sin 2\pi f_s t + a_2 \cos 4\pi f_s t + b_2 \sin 4\pi f_s t + a_3 \cos 6\pi f_s t + b_3 \sin$

$6\pi f_s t$ to the recorded signal, where f_s is the frequency of the suppressor tone. By subtracting the result from the initial signal, the suppressor tone and its first and second harmonic were removed. Next, the signal was digitally filtered using a 60-Hz zero-phase passband filter (amplitude response $A(f) = (1 + [2 \times (f - fcenter)/fwidth]^8)^{-1/2}$). From the Hilbert transform of the filtered signal, the emission frequency of the (partially) suppressed SOAE was computed. In order to further reduce noise, the filtering of the microphone signal was repeated with the filter centered at the computed SOAE frequency and the filter width set to 10 Hz. From the resulting signal, the final estimate of the emission amplitude and frequency was computed. Note that this two-step procedure was chosen instead of a simple single FFT of the signal, followed by picking a single SOAE peak. The procedure outlined here avoids the unfavorable statistical properties of fast Fourier transforms (Press et al., 1992). Sound fragments that contained swallowing or movement noise artefacts, as determined by an artifact level-crossing paradigm, were ignored. Also, recordings for which the suppressor tone was within 10 Hz of the unsuppressed emission frequency were ignored.

The levels of the suppressed SOAEs were ordered in a 21 × 70 or 21 × 27 matrix, where the 70 or 27 columns each contain emission levels for a particular suppression frequency and for a range of suppressor tone levels. Similar matrices were constructed to contain the frequency of the suppressed SOAE. These matrices were smoothed by a 3-point moving average along the level and frequency dimensions. For each frequency, the level at which 3 dB attenuation was reached was computed from the smooth amplitude matrix by linear interpolation between successive tone levels. By combining the results for various frequencies, a 3-dB STC was obtained. These curves show an estimate of the threshold levels needed to obtain 3 dB suppression of the SOAE signal. These tuning curves were characterized by the frequency and level of their minimum (referred to as tip frequency and level) and by their filter quality factors Q_{3dB} and Q_{10dB}. These are defined as the ratio of the tip frequency f_{tip} and the width Δf_{3dB} and Δf_{10dB} of the tuning curve at 3 and 10 dB above the tip frequency: $Q_{3dB} = f_{tip}/\Delta f_{3dB}$ and $Q_{10dB} = f_{tip}/\Delta f_{10dB}$.

As concluded by the Medical Ethics Committee of the University Medical Center Groningen (Letter of 11 March 2014, METc 2014.099), this study it not subject to the Dutch Law Medical-Scientific Research with Humans (Wet Medisch-wetenschappelijk Onderzoek met Mensen, WMO). The study was conducted in accordance with the Declaration of Helsinki and applicable Dutch laws. All subjects gave written, informed consent and received a modest compensation for their participation.

3. Results

3.1. Spontaneous otoacoustic emissions

SOAE were evident as narrow peaks in the sound spectrum recorded in the ear canal. Fig. 1A shows two example SOAE spectra. We report results for 64 SOAE peaks, having frequencies from 0.59 to 14.5 kHz, and level from −8.9 to +16.4 dB SPL. Comparison of the SOAE recordings before and after the suppression measurements only showed small change of SOAE levels (average change −0.1 dB, SD 2.8 dB) and frequency (average change −0.1 Hz, SD 2.8 Hz, average frequency ratio change 0.9999, SD 0.0012).

3.2. Suppression tuning curves and tuning selectivity

We report the following characteristics of the STCs obtained for each of the SOAE being analyzed: the center, or most sensitive, frequency, the tuning selectivity quality factors, the presence and magnitude of facilitation, the presence of secondary suppression dips, the size and direction of frequency shifts and the relationships between these factors.

A sample of the relationship between the amplitude and frequency of the suppressor tone and the SOAE suppression is shown in Fig. 1B, along with the corresponding STC for 3 dB suppression. Fig. 1C shows the collection of all 3-dB STC obtained in the two ears displayed in panel A, including a STC for the subject with the highest SOAE frequency included. The tip, or most sensitive frequency, of the STC was on average 4.5% higher than the frequency of the unsuppressed SOAE peak, and 0.9 (s.d. 5.5) dB above the behavioral tone detection threshold. The STC frequency selectivity was calculated as the filter quality factors Q_{10dB} and Q_{3dB} (tip frequency divided by the bandwidth at 10 dB or 3 dB above tip threshold, respectively). STC values for the two very highest-frequency emissions at 13.8 and 14.5 kHz are not included, since the measurement system did not allow for suppression stimuli at frequencies above 15 kHz. On average, tuning selectivity was moderate (mean $Q_{10dB} = 3.86$, S.D. 1.12) and was independent of the sound pressure level of the unsuppressed SOAE. Remarkably, and in contrast to neural data from other species (Köppl, 1997; Liberman, 1978; Manley et al., 1990; Shera et al., 2011), tuning selectivity showed no dependence on the frequency of the SOAE peaks (Fig. 1D).

3.3. Facilitation, frequency shifting and suppression sidelobes

The behavior of SOAE under suppression conditions was complex. In addition to a main area of suppression (i.e. Fig. 1B), about half of the SOAEs displayed bands of suppression that were sometimes bounded by narrow areas of facilitation and SOAE frequency shifts (see Figs. 2 and 3). These changes were manifest almost exclusively on the high-frequency flanks of STC, with complex patterns of suppression, facilitation and frequency shifting. The most sensitive frequencies of suppression sidelobes were clearly related to the center frequencies of the corresponding STC (Fig. 4A). The sidelobes were also observed in the absence of other SOAE (see Fig. 5 for an example). A sidelobe was observed for 34 SOAE peaks whose center frequencies ranged from 0.621 to 8.781 kHz (Fig. 4). The most sensitive frequencies of these sidelobes were on average 0.56 (s.d. 0.19) octaves above the tip of the main suppression area. For 14 SOAEs, with frequencies ranging from 0.771 Hz to 3.830 kHz, there was an additional secondary sidelobe. The most sensitive frequency of these additional sidelobes was on average 1.03 (s.d. 0.22) octaves above the corresponding main suppression area and 0.56 (s.d. 0.16) above the first sidelobe (Fig. 4B).

Facilitation occurred for 12 SOAE peaks and amounted to up to 6.7 dB. Frequency shifts ranged from −17.6 Hz to +8.3 Hz. Amplitude and frequency changes were related in a complex manner: changes in frequency were approximately proportional to the slope of the amplitude-vs-frequency curve (Fig. 2H). That is, on the low frequency side of a facilitation area, the SOAE frequency increased with stimulus frequency, while on the high-frequency side, the SOAE frequency decreased (See Figs. 2H and 3R).

4. Discussion

Spontaneous otoacoustic emissions in young human subjects showed spectra that strongly resemble those previously published (e.g. Talmadge et al., 1993). As also previously shown, they were suppressed by external tones. The suppression of a SOAE was characterized by a V-shaped main suppression area, with its most sensitive tip just below the emission frequency and tip level close to the psychophysical tone detection threshold. In our large sample,

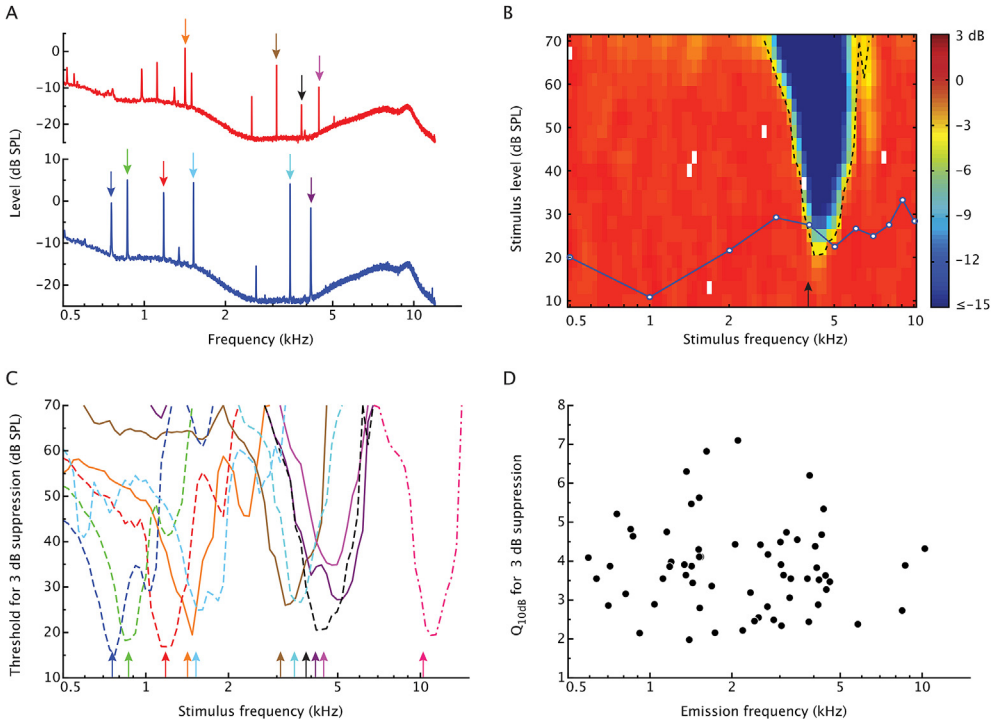

Fig. 1. Suppression of spontaneous otoacoustic emissions (SOAE). (A) Spectra of the SOAE recorded in subject 1 from the right (red curve) and left (blue curve) ears. The peaks in the spectra correspond to faint tones (SOAE) emitted spontaneously from the subject's ears. The arrows indicate emission peaks for which SOAE suppression is illustrated in panels (B) and (C). (B) Suppression of the SOAE at 4.143 kHz (vertical black arrow) from the left ear of subject 1. The colors indicate the amount of suppression produced by stimulus tones having frequencies and levels shown on the horizontal and left vertical axes, respectively. The degree of suppression (negative values) is shown by the colour bar on the right. The white pixels correspond to measurements that were omitted due to a noise artifact. The dashed black contour indicates the suppression tuning curve (STC), showing the stimulus level needed for 3 dB suppression of the SOAE peak. The blue curve with data points is the individual ear's psychoacoustical threshold of hearing, measured during the same experimental session. (C) STCs for 3 dB suppression, measured in the right ear (solid curves) and left ear (dashed curves) of subject 1. The arrows indicate the corresponding SOAE frequencies, with colors matching the arrows in panels (A) and (B). The pink dash-dot curve on the far right was measured in subject 2 and is the highest-frequency STC that was obtained. The black curve is the same as that in panel (B). (D) Filter quality factor Q_{10dB} of all 3 dB suppression contours (n = 64) as determined across 23 ears of 13 subjects. (For interpretation of the references to colour in this figure legend, the reader is referred to the web version of this article.)

Q_{10dB} filter quality factors were remarkably stable across SOAE frequencies. Narrow bands of suppression, facilitation and small frequency shifts were observed for stimulus frequencies above the main suppression area.

Near their center frequency, human SOAE could be suppressed using very low-level tones that lie near behavioral thresholds. This is thus the most sensitive method ever used to systematically measure tuning selectivity across the frequency range of the human cochlea. A comparison of SOAE suppression selectivity and auditory-nerve selectivity is possible in a variety of vertebrate species, but SOAE are rare in both non-primate mammals and birds (Manley, 2001). In the Macaque, the few STC so far measured in this species had center frequencies between 1.39 and 2.38 kHz and Q_{10db} values lay between 5.7 and 10.0 (Martin et al., 1988). These are within the range of neural tuning selectivity data shown by Macaque auditory nerve fibers in this frequency range (neural Q_{10dB} between ~3 and 13; Shera et al., 2011). In various lizard species and in the barn owl, the selectivity Q_{10dB} values of neural and SOAE STC tuning curves are also essentially identical (Köppl, 1997; Köppl and Manley, 1994; Manley et al., 1990; Taschenberger and Manley, 1997). Thus, in macaque, barn owl and in lizards, Q_{10dB} of SOAE STC closely resemble peripheral neural tuning. These data thus suggest that the tuning of SOAE-STC can also be a good proxy for auditory-nerve selectivity in mammals, including humans.

Our frequency selectivity data strongly resemble previous measurements of simultaneous-masking (psychophysical) tuning selectivity in humans (Eustaquio-Martin and Lopez-Poveda, 2010; Lopez-Poveda and Eustaquio-Martin, 2013; Glasberg and Moore, 1990; Baiduc et al., 2014; See Fig. 6a), but do not support the exceptionally high selectivity as assumed from SFOAE phase delays (Shera et al., 2002, 2010, Fig. 4b). Remarkably, the Q_{10dB} values of SOAE STC did not vary with frequency, whereas in all other mammalian species so far studied, the frequency selectivity of auditory neurons rises with center frequency. As a comparison, up to 1–2 kHz, the mean selectivity values in our data tend to be higher than those of cat and Macaque monkey auditory neurons, but, at 10 kHz our STC values are only half those mean neural values (Shera et al., 2011, Fig. 6b).

Charaziak et al. (2013) compared STC measured for SFOAE and behavioral measures of tuning (simultaneous masking psychophysical tuning curves, PTC) in 10 normal-hearing listeners for frequency ranges centered around 1.0 and 4.0 kHz. The probe levels were 10 dB SL for PTC and 20 or 30 dB SL for SOAE-STC. SFOAE STC qualitatively resembled PTC, with similar asymmetric band-pass characteristics, but unlike PTCs they were consistently tuned to frequencies just above the probe frequency. In these respects they strongly resemble the SOAE-STC reported here. Charaziak et al. (2013) suggested that PTCs are predominantly shaped by the frequency-selective filtering and suppressive effects of the cochlea. The $Q10_{dB}$ values reported by these authors for both the SFOAE-STC and the PTC lay between 3.5 and 5.0 for both frequencies investigated and thus in the same range as reported here for SOAE-STC.

There are profound commonalities between SOAE spectral patterns and SFOAE delays in data from lizards, the barn owl and humans. Specifically, the spectral spacing of SOAE correlates well with the phase-delay patterns of SFOAE (Bergevin et al., 2015). The

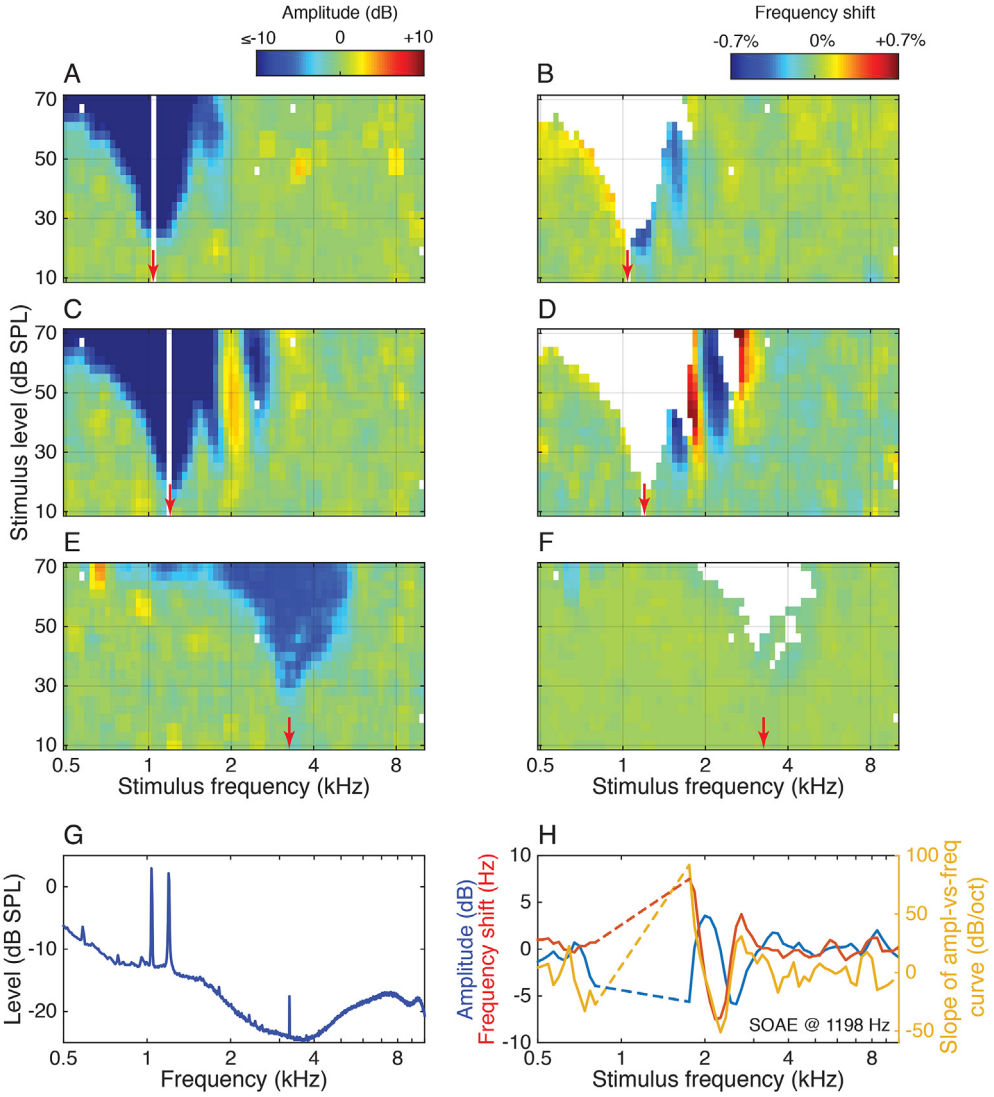

Fig. 2. Suppression tuning (left column) and frequency shifts (right column) for three SOAEs as measured in one ear. (A),(B) SOAE at 1.039 kHz (C),(D) SOAE at 1.198 kHz (E), (F) SOAE at 3.259 kHz. The red arrows on the horizontal axes indicate the unsuppressed SOAE frequency in each case. The map colors indicate the amount of suppression (panels A,C,E) and frequency shift (panels B,D,F) produced by stimulus tones with frequencies and levels shown on the horizontal and left vertical axes, respectively. The white pixels correspond to measurements that were omitted due to a noise artifact or with stimulus frequencies within 10 Hz of the unsuppressed spontaneous emission frequency. In the right column of panels B,D,F, frequency estimates were also masked (white pixels) when the emission amplitude was suppressed by 6 dB or more. (G) Spectrum of the unsuppressed SOAE signal. (H) Amplitudes and frequencies of the SOAE at 1.198 kHz for suppression tones at 49 dB SPL. The panel highlights the relationship between amplitude and frequency shifts of the SOAE, where frequency shifts (red curve) are approximately proportional to the derivative (or slope, orange curve) of the amplitude (blue curve). (For interpretation of the references to colour in this figure legend, the reader is referred to the web version of this article.)

same is true in humans (Zwicker and Peisl, 1990; Shera, 2003; Bergevin et al., 2012). However the tuning selectivity estimated from emission spectral patterns has been shown to be an unreliable predictor of tuning at the level of the auditory nerve in lizard species (Manley et al., 2015). Indeed, a prediction of human frequency selectivity using either SFOAE phase delay data or SOAE spectral peak gap data does not correspond to theSTC selectivity we measured. This, together with human psychoacoustical measurements, suggests that the suppression behavior of SOAE may be a more reliable correlate of auditory-nerve frequency tuning than is the phase behavior of SFOAE or the spectral patterns of SOAE.

Q_{10dB} values from a recent study of humans that used a needle electrode placed through the eardrum to record the selectivity of summed cochlear nerve responses (Verschooten et al., 2015) cannot be adequately compared to previous measures or to our own, since that study used much higher sound pressures (55–75 dB SPL). Isoresponse frequency tuning decreases in bandwidth - and is thus more selective - at higher sound pressures (Eustaquio-Martin and Lopez-Poveda, 2010), making a comparison to threshold-level measurements very unreliable.

Our results display a complexity of the interaction between suppressor tones and SOAE that was not expected on the basis of earlier human suppression reports (Frick and Matthies, 1988; Rabinowitz and Widin, 1984; Schloth and Zwicker, 1983). However, such complexities have been observed in other species (e.g. Köppl and Manley, 1994). While level suppression in humans has been previously reported, facilitation in mammals has only been reported for sound-elicited, but not spontaneous, emissions (e.g. in rabbits, Martin et al., 1987). Our studies were able to show the complex interaction patterns because SOAEs were recorded for a full matrix of stimulus levels and frequencies, rather than only presenting tone levels aimed at producing a pre-defined

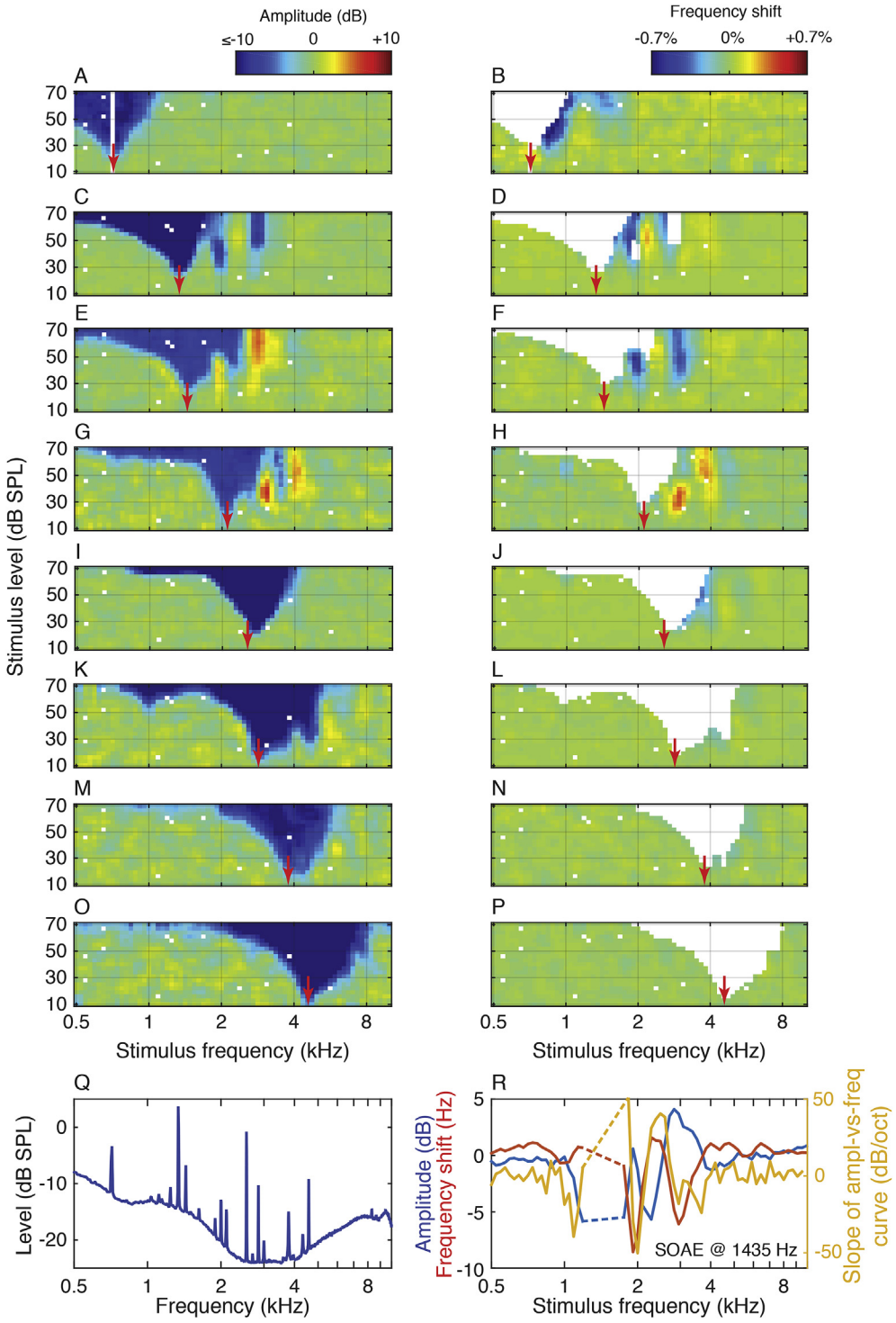

Fig. 3. Suppression tuning and frequency shifts for 8 SOAEs as measured in one ear. (A), (B) SOAE at 0.713 kHz (C), (D) SOAE at 1.337 kHz (E), (F) SOAE at 1.435 kHz (G), (H) SOAE at 2.106 kHz (I), (J) SOAE at 2.545 kHz (K), (L) SOAE at 2.847 kHz (M), (N) SOAE at 3.784 kHz (O), (P) SOAE at 4.580 kHz. The red arrows on the horizontal axes indicate the unsuppressed SOAE frequency. The map colors indicate the amount of suppression (panels A, C, E, G, I, K, M, O) and frequency shift (panels B, D, F, H, J, L, N, P) produced by stimulus tones with frequencies and levels shown on the horizontal and left vertical axes, respectively. The white pixels correspond to measurements that were omitted due to a noise artifact or with stimulus frequencies within 10 Hz of the unsuppressed spontaneous emission frequency. In the right column of panels, frequency estimates were also masked (white pixels) when the emission amplitude was suppressed by 6 dB or more. (Q) Spectrum of the unsuppressed SOAE signal. (R) Amplitude and frequency of the SOAE at 1.435 kHz for suppression tones across the frequency range at 49 dB SPL. The panel shows the relationship between amplitude and frequency shifts of the SOAE, where frequency shifts (red curve) are approximately proportional to the derivative (or slope, orange curve) of the amplitude (blue curve). (For interpretation of the references to colour in this figure legend, the reader is referred to the web version of this article.)

suppression criterion. Like SOAE data from the Macaque monkey, which had STC center frequencies of between 1.39 and 2.06 kHz (Martin et al., 1988), human STC in our collective often showed narrow sidelobes corresponding to highly frequency selective

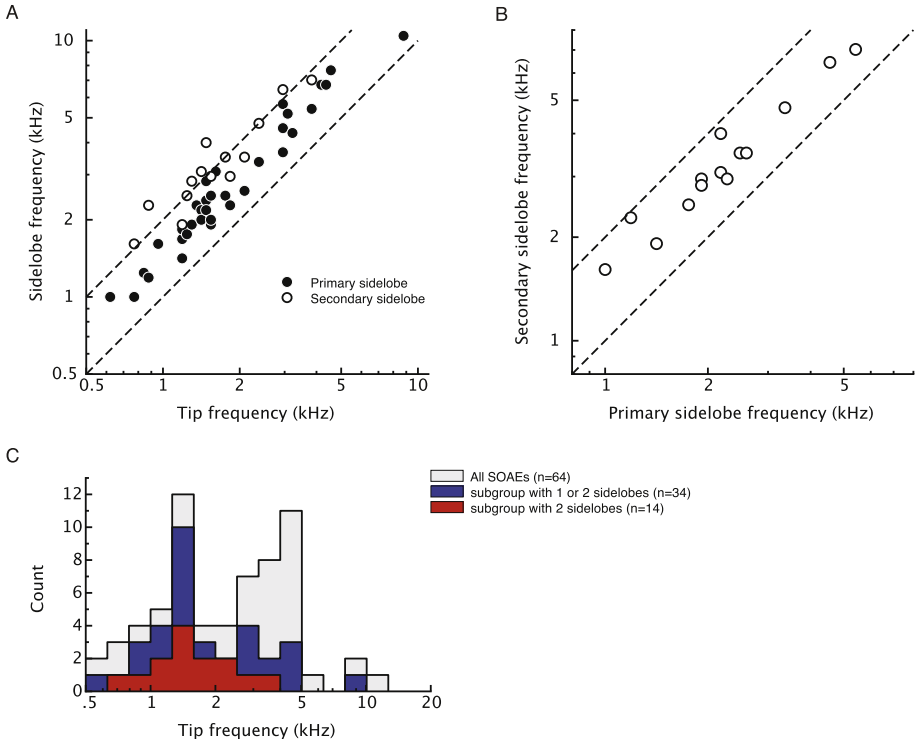

Fig. 4. Frequencies of the sidelobes of SOAE suppression tuning curves. (A) Sidelobe frequency as a function of tip frequency of the tuning curve. Primary (closed symbols; n = 34) and secondary (open symbols; n = 14) sidelobe values are shown. (B) Primary as a function of secondary sidelobe frequencies for the subset of suppression tuning curves where 2 sidelobes were observed. The dashed diagonal lines in both panels are added for orientation and are 1 octave apart. (C) Distribution of tip frequencies of all SOAE tuning curves obtained in this work. Grey: all tuning curves. Blue: subgroup of tuning curves with one side lobe. Red: subgroup of tuning curves with two side lobes. (For interpretation of the references to colour in this figure legend, the reader is referred to the web version of this article.)

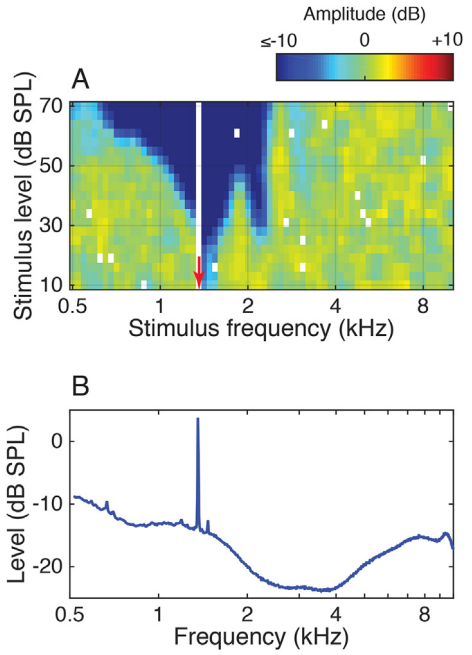

Fig. 5. Secondary lobe in the absence of corresponding other SOAE peaks. Suppression tuning measured in an ear with one strong spontaneous emission. (A) Amount of suppression as a function of frequency and level. (B) Spectrum of the unsuppressed emission signal. Panel A shows a side lobe above the main suppression area (tip frequency 1414 Hz) near 2.2 kHz, even though there is no SOAE peak anywhere near the side lobe.

suppression for stimulus frequencies above the main suppression area. In fact, one human study showed a small high-frequency suppression dip in a human STC (Zwicker and Peisl, 1990). Such sidelobes are quite common in lizard SOAE-STC, as is facilitation and frequency shifting (e.g. Köppl and Manley, 1994). In the species for which most data are available, the Bobtail skink *Tiliqua rugosa*, such secondary sensitivity dips on the high-frequency flanks were also observed in auditory-nerve tuning curves (Manley et al., 1990). However, secondary dips are not routinely observed in mammalian neural tuning curves, as is exemplified by their absence in auditory-nerve tuning curves as compared to SOAE-STC of the Macaque (Martin et al., 1988; Shera et al., 2011). In our data, they are associated with small shifts (<10 Hz) in SOAE frequency and/or mild facilitation of SOAE level (up to 6.7 dB). Thus in mammals, at least, such secondary dips apparently reflect phenomena that are eliminated prior to processing at the neural stage. This, together with a comparison of SOAE-STC selectivity compared to SFOAE phase data suggests that not all phenomena measurable in emissions are reflected in neural activity.

Secondary suppression lobes can be considered to support the hypothesis that SOAEs are standing waves on the basilar membrane in the inner ear. The possible involvement of standing waves had been suggested (e.g. Kemp, 1980; Shera, 2003) but did not yet find direct support. The idea was explicitly explored by Epp et al. (2015). In an active nonlinear transmission line model of the human cochlea, they showed that a single SOAE peak corresponds to a cochlear travelling wave that peaks at the tonotopic location of the emission frequency but, in addition, generates a standing wave on the basilar membrane that lies basal to the tonotopic place (See Fig. 7). This standing wave has antinodes along the basilar membrane. The two antinodes closest to the tonotopic location of the

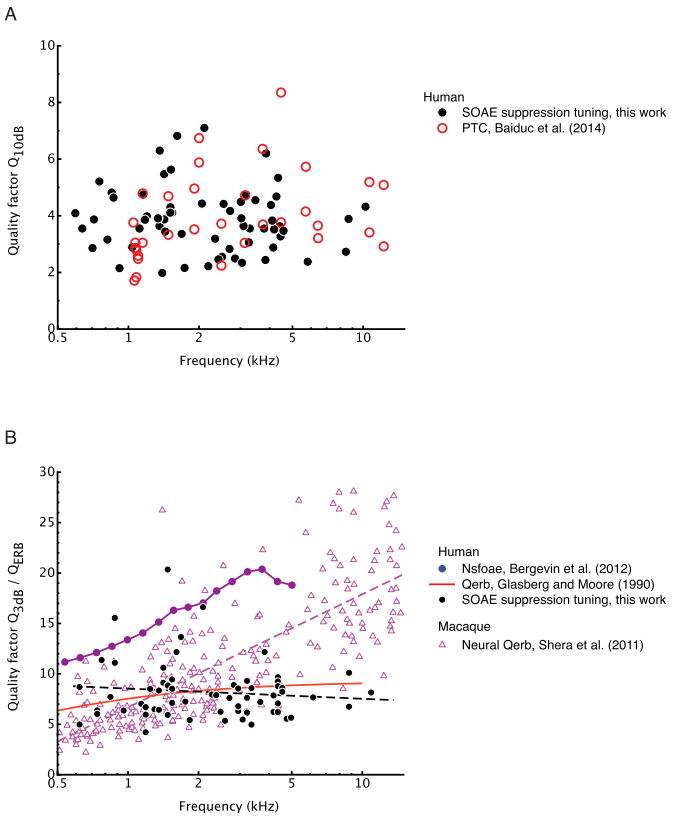

Fig. 6. Comparison between filter quality measures and species. (A) Filter quality factor Q_{10dB} in humans as determined from suppression tuning curves (STC) of spontaneous otoacoustic emissions (SOAE, filled black symbols, this work) and from human psychophysical tuning curves (open red symbols, Baiduc et al., 2014). (B) The filter quality factor for SOAE suppression tuning curves shown again (filled black symbols), now as Q_{3dB} to allow easy comparison to other measures in the panel. These measures are the phase gradient N_{SFOAE} as determined using 20 dB SPL stimuli in human subjects (closed purple symbols, Bergevin et al., 2012), the equivalent rectangular band Q_{erb} of psychophysical masking in humans (red curve, derived from Fig. 7 in Glasberg and Moore, 1990), and neural Q_{erb} obtained in the Macaque auditory nerve (open magenta triangles, Shera et al., 2011). The dashed black curve is a logarithmic linear fit to the human SOAE tuning data with slope −0.30 (±0.35) oct^{-1}. The magenta dashed curve is a similar fit to the Macaque neural data with slope +3.4 (±0.2) oct^{-1}. (For interpretation of the references to colour in this figure legend, the reader is referred to the web version of this article.)

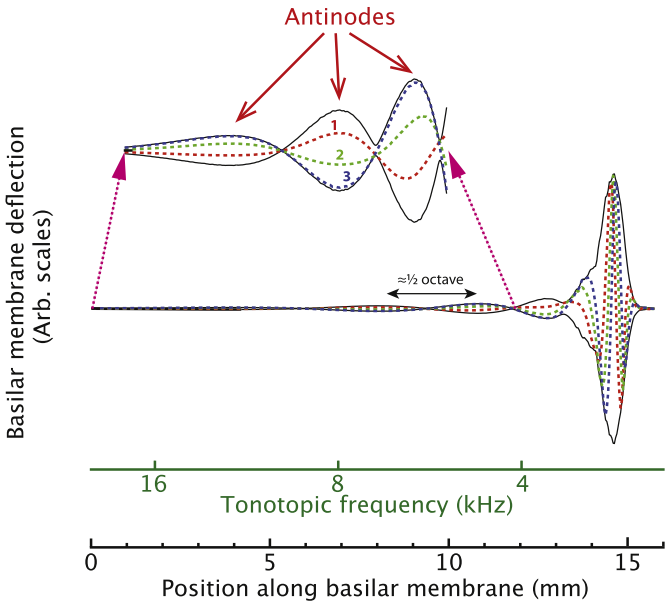

Fig. 7. Modeled basilar membrane motion corresponding to the activity produced by a SOAE at 2.6 kHz (adapted from Fig. 4b from Epp et al., 2015). The nonlinear active transmission line model of the cochlea by Epp et al. shows spontaneous activity on the basilar membrane that contains several narrowband components. Filtering out a single component reveals the activity along the basilar membrane that corresponds to a single SOAE peak generated by the model, in this case corresponding to a SOAE peak at 2.6 kHz. The motion pattern for 2.6 kHz peaks at the 2.6-kHz tonotopic place, and is a travelling wave on the basilar membrane (apical to position x ≈ 13 mm). Basal to the peak region (e.g. basal to x ≈ 12 mm), a standing wave is present. The standing wave has antinodes at tonotopic locations about a ½ octave apart. The high-frequency sidelobes in SOAE suppression patterns (i.e. Fig. 2, panel A and C; Fig. 5, panel A) may reflect the interaction between high-frequency suppressor tones and antinodes of the standing wave. See main text. The horizontal axes display distance from the stapes (black) and tonotopic frequency (green). The inset above shows the portion of that basilar membrane that exhibits a standing wave. In the inset, the vertical axis was expanded to highlight the antinodes of the standing wave. The colored dashed curves show the position of the basilar membrane at subsequent moments in time: The solid black curves display the envelope of the oscillation pattern. See the online supplemental material for animations of the basilar membrane vibration pattern. (For interpretation of the references to colour in this figure legend, the reader is referred to the web version of this article.)

SOAE are at the tonotopic places tuned approximately ½ and 1 octave above the SOAE frequency. We propose that a high-frequency suppressive tone interacts with the standing wave. If the tone peaks at an SOAE antinode, it suppresses the standing wave and hence the emission signal. This would account for the suppressive sidelobes in SOAE suppression tuning curves as we found, which are approximately ½ and 1 octave above the emission frequency. In other words, external tones with frequencies above an SOAE probe the antinodes of emission-related cochlear standing waves. Note that this explanation is analogous to the creation of flageolette tones on a violin: by lightly pressing the string on the violin key, vibrations with antinodes at the finger location are selectively suppressed, thus removing some lower harmonics from the violin sound. In the cochlea, the role of the pressing finger is played by the external suppressing tone, which selectively suppresses an SOAE frequency by nonlinear interaction with the standing wave on the basilar membrane. Although this provides a straightforward interpretation of the sidelobes in SOAE suppression tuning curves, these phenomena were also observed in SOAE-STC measured in various lizard species. Since lizard papillae lack a travelling wave along the basilar membrane (Manley et al., 1989), standing waves will not be possible and further investigation is needed to examine whether the sidelobes in various species represent manifestations of the same phenomena.

The Q_{10dB} estimates are not affected by the secondary dips, since they do not influence the slope within 10 dB of the most sensitive tip. Mammalian cochlear processing up to the primary neural level has, compared to lizards at least, apparently eliminated the complexities of secondary sensitivity dips, resulting in the smooth and steep high-frequency flanks of neural tuning curves.

A direct comparison of human SFOAE to the present data reveals a profound difference between them (Fig. 6B). For this comparison, we used the Q_{3dB} sharpness coefficient of our STC, which is roughly equivalent to the Q_{erb} commonly used in SFOAE studies (in the barn owl, $Q_{erb}/Q_{3dB} = 0.9$; C. Köppl, pers. comm). If we are correct in assuming that our STC match human neural tuning, then the relationship of neural tuning to SFOAE delays (Fig. 6B) is not a direct or even frequency-invariant one. Possibly, this is related to the complicated relation between SFOAE delay and tuning sharpness as shown in nonlinear transmission line models of the cochlear (Sisto and Moleti, 2015). This throws strong doubt on the use of SFOAE delays as a reliable predictor of neural selectivity.

Comparing our tuning data from human STC to auditory-nerve data from the cat, guinea pig and Macaque monkey indicates that

up to 1–2 kHz, human tuning is sharper, but above 2 kHz, it is less sharp, and is, in total, unusually independent of frequency. An example comparing Macaque neural data is shown in Fig. 6B. The somewhat higher frequency selectivity below 2 kHz in humans can speculatively be interpreted as a possible adaptation to the main frequencies used in speech. It can even be speculated that the spatial distribution of frequency in the human cochlea is not simply logarithmic, with equal space available for each octave, but instead may devote more space to lower frequency octaves. Recent genetic evidence indicates that in the human lineage, our ancestors " ….show cochlear relative lengths and oval window areas larger than expected for their body mass, two features corresponding to increased low-frequency sensitivity more recent than 2 million years ago" (Braga et al., 2015). These changes are likely to have been the result of selection for cochleae in which the length increase improved low-frequency hearing and which were thus better able to process increasingly complex and differentiated human communication signals. One result of these changes might be the unique pattern of frequency selectivity we observed in STC of SOAE.

With regard to spectral patterns (as distinct from tuning selectivity) of SOAE, in various lizard species and in the barn owl, the relationship between selectivity derived from the frequency spacing of SOAE on the one hand and neural tuning selectivity on the other varies from near 1:1 to up to 5:1 (Manley et al., 2015). Thus in some species, neural tuning does reflect the apparent maximal tuning selectivity offered by the cochlear hair-cell system, as perhaps seen in the frequency spacing of SOAE (Manley et al., 2015) and in SFOAE patterns (Bergevin et al., 2015). In other species, by contrast, including humans, this is apparently not the case and neural tuning is much less sharp at higher frequencies. It thus remains a challenge to understand and to model the factors that determine the inconsistent relationship between SFOAE, STC of SOAE and neural data. Our data in humans and comparable data from other species show that the relationship between pre-neural mechanical processing in the cochlea (SOAE, SFOAE) and neural coding at the hair-cell/auditory nerve synapse is still incompletely understood.

In conclusion, suppression of spontaneous otoacoustic emissions is frequency selective, with most sensitive suppression close to the emission frequency. The V-shaped suppression tuning curves show a filter quality that is independent of frequency. Filter quality is consistent with psychoacoustical simultaneous masking tuning measures. At high frequencies it is very modest in comparison to quality estimates based on stimulus frequency otoacoustic emissions. Many spontaneous emissions are also suppressed by tones at about ½ and 1 octave above the emission frequency, possibly due to suppression of an emission-related standing wave on the basal portion of the basilar membrane.

Supplementary data related to this article can be found online at http://dx.doi.org/10.1016/j.heares.2016.04.004.

Author contributions

G.A.M. and P.v.D. designed research; P.v.D. performed research; G.A.M. and P.v.D. analyzed data; G.A.M., and P.v.D. wrote the paper.

Conflicts of interest

The authors declare no conflict of interest.

Acknowledgements

We thank C. Köppl, U. Sienkecht, A. Maat and E. de Kleine for discussions and support. PvD was supported by the Heinsius Houbolt Foundation. We thank B. Epp for providing the material used to generate Fig. 7.

References

Baiduc, R.R., Lee, J., Dhar, S., 2014. Spontaneous otoacoustic emissions, threshold microstructure, and psychophysical tuning over a wide frequency range in humans. J. Acoust. Soc. Am. 135, 300–314.
Bergevin, C., Fulcher, A., Richmond, S., Velenovsky, D., Lee, J., 2012. Interrelationships between spontaneous and low-level stimulus-frequency otoacoustic emissions in humans. Hear. Res. 285, 20–28.
Bergevin, C., Manley, G.A., Köppl, C., 2015. Salient features of otoacoustic emissions are common across tetrapod groups and suggest shared properties of generation mechanisms. Proc. Nat. Acad. Sci. U. S. A. 112, 3362–3367.
Braga, J., Loubes, J.-M., Descouens, D., Dumoncel, J., Thackeray, J.F., Kahn, J.-L., de Beer, F., Riberon, A., Hoffman, K., Balaresque, P., Gilissen, E., 2015. Disproportionate cochlear length in genus homo shows a high phylogenetic signal during apes' hearing evolution. PLoS One 10 (6), e0127780. http://dx.doi.org/10.1371/journal.pone.0127780.
Charaziak, K.K., Souza, P., Siegel, J.H., 2013. Stimulus-frequency otoacoustic emission suppression tuning in humans: comparison to behavioral tuning. JARO 14, 843–862.
Epp, B., Wit, H.P., Van Dijk, P., 2015. Clustering of cochlear oscillations in frequency plateaus as a tool to investigate SOAE generation. In: Karavitaki, K.D., Corey, D.P. (Eds.), Mechanics of Hearing: Protein to Perception, Proceedings of the 12th International Workshop on the Mechanics of hearing. AIP Conf. Proc., 1703, p. 090025.
Eustaquio-Martin, A., Lopez-Poveda, E.A., 2010. Isoresponse versus isoinput estimates of cochlear filter tuning. J. Assoc. Res. Otolaryngol. 12, 281–299.
Frick, L.R., Matthies, M.L., 1988. Effects of external stimuli on spontaneous otoacoustic emissions. Ear Hear. 9, 190–197.
Glasberg, B.R., Moore, B.C.J., 1990. Derivation of auditory filter shapes from notched-noise data. Hear. Res. 47, 103–138.
Kemp, D.T., 1978. Stimulated acoustic emissions from within the human auditory system. J. Acoust. Soc. Am. 64 (5), 1386–1391.
Kemp, D.T., 1980. Towards a model for the origin of cochlear echoes. Hear. Res. 2, 533–548.
Köppl, C., 1997. Frequency tuning and spontaneous activity in the auditory nerve and cochlear nucleus magnocellularis of the barn owl Tyto alba. J. Neurophysiol. 77, 364–377.
Köppl, C., Manley, G.A., 1994. Spontaneous otoacoustic emissions in the bobtail lizard. II: interactions with external tones. Hear. Res. 72, 159–170.
Liberman, M.C., 1978. Auditory-nerve response from cats raised in a low-noise chamber. J. Acoust. Soc. Am. 63, 442–455.
Lopez-Poveda, E.A., Eustaquio-Martin, A., 2013. On the controversy about the sharpness of human cochlear tuning. J. Assoc. Res. Otolaryngol. 14, 673–686.
Manley, G.A., 2001. Evidence for an active process and a cochlear amplifier in nonmammals. J. Neurophysiol. 86 (2), 541–549.
Manley, G.A., Köppl, C., Yates, G.K., 1989. In: Wilson, J.P., Kemp, D. (Eds.), Micromechanical Basis of High-frequency Tuning in the Bobtail Lizard. Mechanics of Hearing. Plenum, New York, pp. 143–150.
Manley, G.A., Köppl, C., Johnstone, B.M., 1990. Peripheral auditory processing in the bobtail lizard Tiliqua rugosa: I. Frequency tuning of auditory-nerve fibres. J. Comp. Physiol. A 167, 89–99.
Manley, G.A., Köppl, C., Bergevin, C., 2015. Common substructure in otoacoustic emission spectra of land vertebrates. In: Karavitaki, K.D., Corey, D.P. (Eds.), Mechanics of Hearing: Protein to Perception, Proceedings of the 12th International Workshop on the Mechanics of hearing. AIP Conf. Proc., 1703, p. 090012.
Martin, G.K., Lonsbury-Martin, B.L., Probst, R., Scheinin, S.A., Coats, A.C., 1987. Acoustic distortion products in rabbit ear canal. II. Sites of origin revealed by suppression contours and pure-tone exposures. Hear. Res. 28, 191–208.
Martin, G.K., Lonsbury-Martin, B.L., Probst, R., Coats, A.C., 1988. Spontaneous otoacoustic emissions in a nonhuman primate. I. Basic features and relations to other emissions. Hear. Res. 33, 49–68.
Press, W.H., Teukolsky, S.A., Vetterling, W.T., Flannery, B.P., 1992. Numerical Recipes in C, second ed. Cambridge University Press, Cambridge.
Rabinowitz, W.M., Widin, G.P., 1984. Interaction of spontaneous oto-acoustic emissions and external sounds. J. Acoust. Soc. Am. 76, 1713–1720.
Ruggero, M.A., Temchin, A.N., 2005. Unexceptional sharpness of frequency tuning in the human cochlea. Proc. Nat. Acad. Sci. U. S. A. 102, 18614–18619.
Schloth, E., Zwicker, E., 1983. Mechanical and acoustical influences on spontaneous oto-acoustic emissions. Hear. Res. 11, 285–293.
Shera, C.A., 2003. Mammalian spontaneous otoacoustic emissions are amplitude-stabilized Cochlear standing waves. J. Acoust. Soc. Am. 114, 244–262.
Shera, C., Guinan, J.J., Oxenham, A.J., 2002. Revised estimates of human cochlear tuning from otoacoustic and behavioral measurements. Proc. Nat. Acad. Sci. U. S. A. 99, 3318–3323.
Shera, C., Guinan, J.J., Oxenham, A.J., 2010. Otoacoustic estimation of Cochlear tuning: validation in the Chinchilla. J. Assoc. Res. Otolaryngol. 11, 343–365.
Shera, C.A., Bergevin, C., Kalluri, C.R., McLaughlin, M., Michelet, P., van der Heijden, M., Joris, P.X., 2011. Otoacoustic estimates of cochlear tuning: testing predictions in macaque. In: Shera, C.A., Olson, E.S. (Eds.), What Fire is in My Ears: Progress in Auditory Biomechanics. American Institute of Physics, AIP Conf Proc., 1403, pp. 286–292.
Siegel, J.H., 2007. Calibration of otoacoustic emission probes. In: Robinette, M.S.,

Glattke, T.J. (Eds.), Calibration of Otoacoustic Emission Probes. Otoacoustic Emissions: Clinical Applications, third ed. Thieme, New York, pp. 403–428.
Siegel, J.H., Cerka, A.J., Recio-Spinoso, A., Temchin, A.N., van Dijk, P., Ruggero, M.A., 2005. Delays of stimulus-frequency otoacoustic emissions and cochlear vibrations contradict the theory of coherent reflection filtering. J. Acoust. Soc. Am. 118, 2434–2443.
Sisto, R., Moleti, A., 2015. On the dependence of the BM gain and phase on the stimulus level. In: Karavitaki, K.D., Corey, D.P. (Eds.), Mechanics of Hearing: Protein to Perception, Proceedings of the 12th International Workshop on the Mechanics of hearing. AIP Conf. Proc., 1703, p. 070007.
Talmadge, C.L., Long, G.R., Murphy, W.J., Tubis, A., 1993. New off-line method for detecting spontaneous otoacoustic emissions in human subjects. Hear. Res. 71, 170–182.
Taschenberger, G., Manley, G.A., 1997. Spontaneous otoacoustic emissions in the barn owl. Hear. Res. 110, 61–76.
van Dijk, P., Maat, B., de Kleine, E., 2011. The effect of static ear canal pressure on human spontaneous otoacoustic emissions: spectral width as a measure of the intra-cochlear oscillation amplitude. Hear. Res. 12, 13–28.
Verschooten, E., Desloovere, C., Joris, P.X., 2015. Human neural tuning estimated from compound action potentials in normal hearing human volunteers. In: Karavitaki, K.D., Corey, D.P. (Eds.), Mechanics of Hearing: Protein to Perception, Proceedings of the 12th International Workshop on the Mechanics of hearing. AIP Conf. Proc., 1703, p. 070001.
Zurek, P.M., 1981. Spontaneous narrowband acoustic signals emitted by human ears. J. Acoust. Soc. Am. 69, 514–523.
Zwicker, E., Peisl, W., 1990. Cochlear preprocessing in analog models, in digital models and in human inner ear. Hear Res. 44, 209–216.